LASER INTERFEROMETER GRAVITATIONAL WAVE OBSERVATORY
- LIGO -
CALIFORNIA INSTITUTE OF TECHNOLOGY
MASSACHUSETTS INSTITUTE OF TECHNOLOGY

September 17th, 2016

Developing Features for Gravitational Wave Detector Characterization

Author: Praful Vasireddy
Mentors: Maximiliano Isi, Gautam Venugopalan, Rana Adhikari

California Institute of Technology
LIGO Project, MS 18-34
Pasadena, CA 91125
Phone (626) 395-2129
Fax (626) 304-9834
E-mail: info@ligo.caltech.edu

Massachusetts Institute of Technology
LIGO Project, Room NW22-295
Cambridge, MA 02139
Phone (617) 253-4824
Fax (617) 253-7014
E-mail: info@ligo.mit.edu

LIGO Hanford Observatory
Route 10, Mile Marker 2
Richland, WA 99352
Phone (509) 372-8106
Fax (509) 372-8137
E-mail: info@ligo.caltech.edu

LIGO Livingston Observatory
19100 LIGO Lane
Livingston, LA 70754
Phone (225) 686-3100
Fax (225) 686-7189
E-mail: info@ligo.caltech.edu

http://www.ligo.caltech.edu/

Abstract

This project consisted of developing new tools for gravitational wave detector characterization by making use of data obtained from the 40m LIGO interferometer at Caltech. The purpose of detector characterization is to provide an understanding of noise sources and convey information about the state of a detector and its surroundings. This knowledge is fundamental to distinguish an astrophysical signal from noise and thus make a detection. This project contributed to such efforts by creating a system to display MEDM status and control screens on online summary pages to give more physical context to data and allow for easier debugging. Additionally, this project also developed a system to measure the acoustic noise of the interferometer to further improve detector characterization. The future goal will be to set up multiple microphones and amplifiers along the interferometer to eventually study the coupling of acoustic noise to the differential arm length of the interferometer. Furthermore, a new tab for the acoustic noise measurement has been added to the online summary pages.

Contents

1 Background

1.0.1 Basics of General Relativity

In 1915, Einstein published his theory of general relativity which described gravitational forces as the curvature of four-dimensional spacetime. He found that the effects of gravity on a particle can be explained as resulting from its movement in a geodesic, a "straight line" in curved spacetime. Furthermore, similar to the radiation of electromagnetic waves from accelerating charges, Einstein found that the vacuum solutions to his field equations supported waves of oscillating strains in spacetime, travelling at the speed of light [7]. However, unlike dipolar electromagnetic waves, gravitational radiation is quadrupolar, meaning that the waves compress spacetime in one direction and elongate it in a plane perpendicular to the direction of motion. The quadrupolar nature of gravitational waves can be derived from the multipole expansion of a system's distribution of mass, as both the monopole and dipole terms must be eliminated due to conservation of mass and conservation of linear and angular momentum, respectively. Although any accelerating mass quadrupole produces gravitational radiation, the amplitude of this gravitational strain is very small, on the order of 10^{-21}, and thus difficult to measure.

1.0.2 LIGO Operation and the Caltech 40m

Advances in technology from Einstein's time have allowed for the detection of gravitational waves to become a reality, as seen through the first direct observation of gravitational radiation, event GW150914, by Advanced LIGO on September 14th, 2015 [1]. The Advanced LIGO detectors are extremely precise modified Michelson interferometers (see Figure 1) which measure the changes in the length of the 4-km-long arms of the interferometer by determining the phase shift of the light from the different arms upon recombination. The central component of the interferometer consists of a 50/50 beam splitter that is illuminated by a laser source. The transmitted and reflected beams travel through perpendicular paths and are reflected by end mirrors to recombine at the beam splitter. Because strain is inversely proportional to the original length, increasing the length of the arms has the effect of increasing the strain sensitivity of the interferometer. However, as increasing the length of the arms indefinitely is not feasible due to terrestrial constraints, mechanisms for effectively lengthening the interferometer are used. Fabry-Perot cavities are used to increase the path length of the light and effectively lengthen the arms of the interferometer [5].

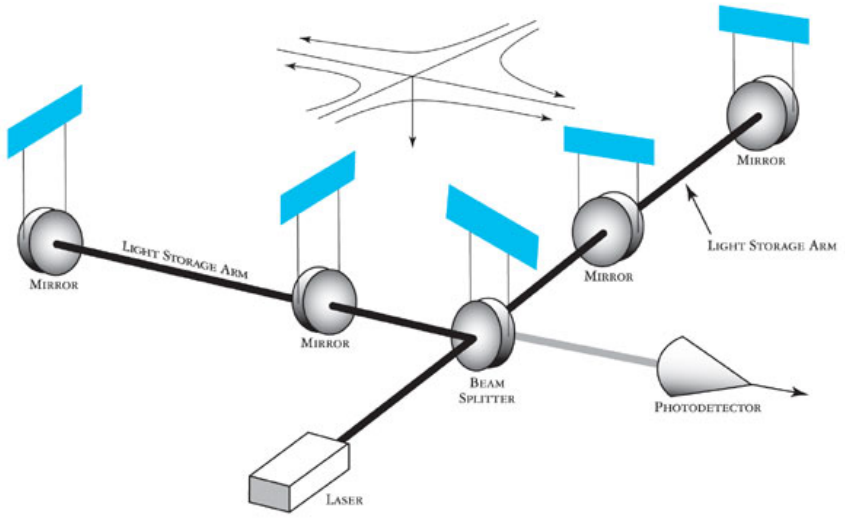

Figure 1: Advanced LIGO optical setup [6]. The arms of the interferometer are 4 km long but the distance the light travels is increased using Fabry-Perot cavities.

The Caltech 40m interferometer operates in a similar manner although the length of the arms is 100 times smaller. This instrument is used as a small-scale prototype for the larger detectors in Hanford, Washington, and Livingston, Louisiana. If new features added to the data analysis or instrument operation procedures of the Caltech 40m are successful, they may be implemented into the larger interferometers.

1.0.3 Noise in LIGO and Detector Characterization

However, because of their extreme sensitivity, the LIGO interferometers have many noise sources due to both the external environment and inherent disturbances from the experimental design. These noises are categorized as either displacement noises which directly move the suspended mirrors or sensing noises which affect the readout signal without actually moving the mirrors. Some forms of displacement noise are seismic noise, thermal noise, and noise caused by radiation pressure resulting from variations in the power of the input laser source. A few examples of sensing noise are laser amplitude noise caused by power fluctuations, noise from vacuum fluctuations entering the interferometer, and readout noise from the electronics themselves. By effectively characterizing these sources of error and observing the signals caused by them, the LIGO operation is made possible. Without being able to determine which parts of a signal are significant and which are the results of noise, no useful data can be obtained.

1.0.4 Applications of LIGO Observations

Detection of gravitational wave signals is useful for applications in gravitational wave astronomy as well as for improving our understanding of gravity. Just as the ability to detect forms of electromagnetic radiation outside the visible spectrum provided numerous insights into astrophysical processes that could not be observed through visible light, gravitational radiation is able to penetrate regions of space that even electromagnetic radiation cannot. Therefore, an improved ability to detect gravitational waves would allow for a greater understanding

of processes such as the merging of black holes or the evolution of binary neutron star systems. Furthermore, studying gravitational wave signals will likely lead to the discovery of astrophysical processes whose existence researchers are currently unaware of. Additionally, detecting gravitational waves allows for confirmations of the predictions of general relativity, a theory which is very difficult to test in a lab setting. However, by analyzing signals and producing simulations, gravitational wave detection functions as a technique to study general relativity using the universe as the laboratory.

2 Objectives and Approach

2.1 Summary Pages

Because the status of the Advanced LIGO detectors is constantly changing, detector characterization is required to change along with it. Thus, the mechanisms used to provide information about the detectors, such as summary pages, must be regularly improved and enhanced with new features. Currently, the 40m detector summary pages are updated twice per hour using a cronjob, a scheduled execution of a shell command, called `gw_summary`. HTCondor, a parallel computing utility which allows many computers to process the data at once, is also used in order to generate daily pages from large amounts of data. The pages are generated by using the `gw_summary` command line executable to parse given configuration files with the .ini format and produce .html files. The configuration (.ini) files consist of a series of key-value pairs which determine the characteristics of the pages, such as what types of plots are included, the layout of the plots, the data channels used, and more [14]. After being written to a .html file, these summary pages display in a browser information through plots from numerous auxiliary channels which describe the state of the detector and its environment, along with the gravitational wave strain data [2, 3]. The pages are currently used by people who work at the Caltech 40m on improving the interferometer and people in detector characterization, in both cases mainly for the purpose of quickly diagnosing issues. An example of the current state of the summary pages is given below in Figure 2, which shows a plot from the July 7, 2016 page.

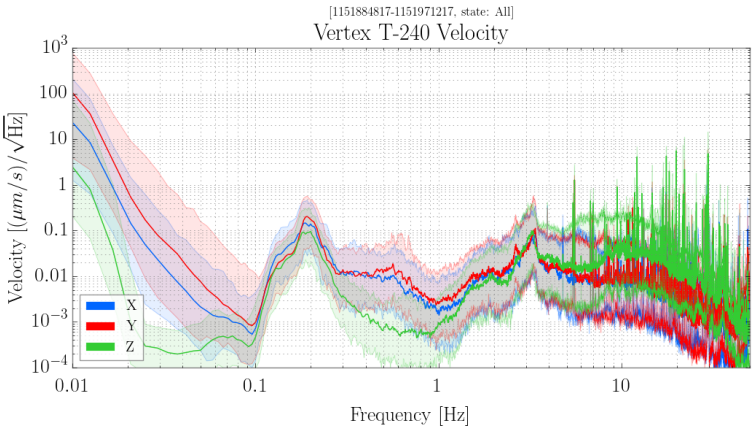

Figure 2: Physical environment monitoring (PEM) seismic data from July 7th [11]. This plot displays spectra of seismic motion at the beam splitter.

2.2 MEDM Tab

One goal of this project was to create a new tab on the data summary pages for MEDM status screens for the interferometer. These screens allow researchers to easily get information about the state of specific parts of the interferometer and make changes from a computer interface. A typical MEDM screen is shown below.

Figure 3: CDS FE STATUS MEDM screen from the 40m. This screen conveys information about the health of the 40m Realtime Control Front-End Machines.

A limitation of the summary pages is that, when data goes awry or does not make sense, there was previously not a great deal of information regarding the physical state of the detector and the parameter settings of its components. This was helped by implementing an automatically-updating new tab which displays screenshots of important MEDM screens on the summary pages. This new feature will hopefully increase the usage of the summary pages at the 40m and give the data more context. To create this new tab, scripts written by Yoichi Aso, a former researcher at the 40m, were modified and formatted to upload screenshots to the summary pages. These scripts had been previously set up to take automated screenshots of the MEDM screens but their use has been discontinued. I succeeded in getting these scripts to run from the current network setup and figuring out how to get the summary pages to include these screenshots.

2.3 Acoustic Noise Cancellation

2.3.1 Motivation and Requirements

Acoustic noise is at a different frequency band than seismic noise, and thus there is a need for a system that effectively reduces the effect of acoustic noise. As such, the goal of this project will be to develop a system to cancel acoustic noise from interferometer readout, specifically the differential arm length channel, which is where gravitational wave strain data appears. Some known noise sources that may couple into the interferometer readout are electronics racks, AC units, and fans.

In order to accomplish this, the system must fit some requirements. First, there needs to be an amplification system in order to ensure that the acoustic signal can be seen. Next, there must be a bandpass filter in this amplification circuit because microphones have a dynamic frequency range determined by mechanical properties. Additionally, the microphones must be held in place somehow and must be isolated. For these last two requirements, a suspended box can be used.

2.3.2 Box Design and Microphone Layout

Suspending a box removes noise in the acoustic signal from both seismic activity as well as wind. If the box has enough weight, it will not oscillate much above the natural frequency determined by the mass of the box and the spring constant of the suspension material. Thus, by choosing the right suspension material and box, the system can be seismically isolated. Surgical tubing has been chosen as a preliminary suspension material due to its rigidity. Additionally, having a heavier box also reduces motion fom wind due to AC units. A preliminary design for the box is given below in Figure 4.

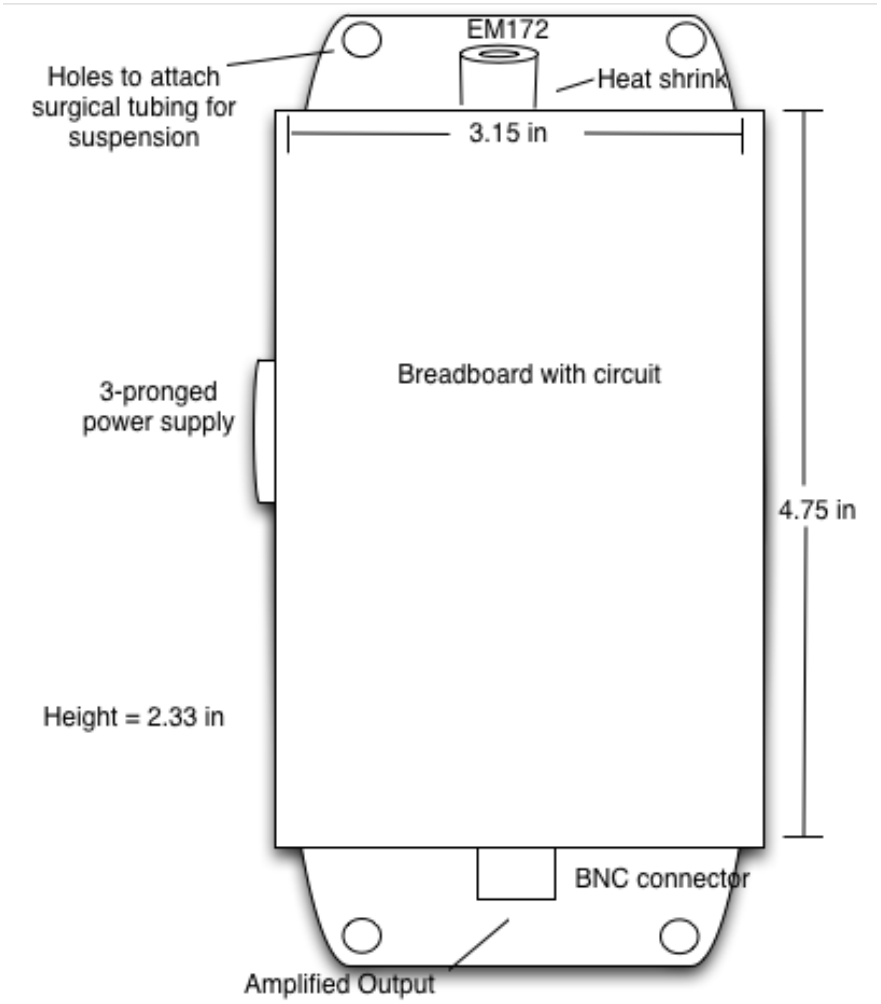

Figure 4: Bottom view of preliminary design for individual microphone amplifier boxes. Surgical tubing will be used to suspend the box and heat shrink will be used to help connect the microphones directly to each circuit.

It is also important to have an array of microphones around the interferometer because it becomes easier to distinguish between noise and true signal and it can pick up acoustic signals that a single microphone cannot. It is not entirely clear yet how to optimize the locations of the microphones, and this process will likely involve some trial and error in order to study the tradeoff between measuring the acoustic signal near the known noise sources or near important areas along the interferometer. However, the current plan is to place microphone-amplifier systems near the ends and midpoints of both arms, electronics racks along both arms, the AS port table, the PSL table, MC2, and the vacuum pumps along the x-arm.

2.3.3 Previous Work

The following circuit schematic was used by previous graduate students at the 40m, although there were some possible issues and elements that seemed like they could be improved.

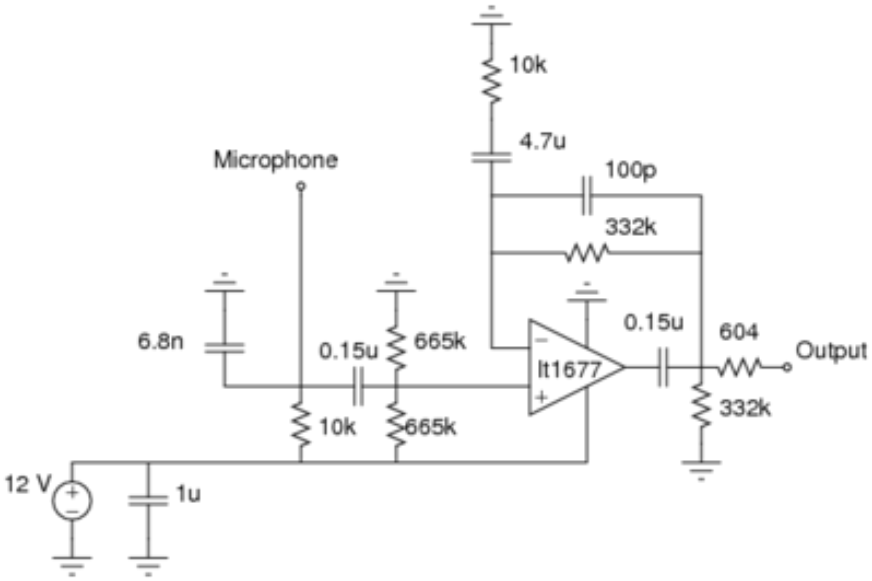

Figure 5: Original circuit schematic by Denis Martynov. Pin 4 from the LT1677 goes to ground rather than being given a negative input voltage. This cuts the range of the opamp in half, which may not be an issue if the signal is completely positive.

Previously, the setup consisted of placing six microphones around the interferometer and connecting them all back to the same amplifier box, which contained six copies of the above circuit, and then reading out the data. However, this system may have resulted in more noisy data due to having the unamplified signal travel a long distance to the amplifier box. To the unamplified signal, noise in signal travel could be relatively large. This noise would then be amplified and could make distinguishing between noise and signal difficult. This problem can be avoided by amplifying directly at the microphone so that less noise is picked up and amplified. To do this, I will be making individual amplifier boxes to which each microphone can be mounted. This hardware will be placed at locations around the interferometer to reduce some signal travel time. I will be putting a single one of my modified amplifier circuits in each new amplifier box. The end goal of this project will be to have data channels set up to measure the acoustic noise at locations around the interferometer and to include a new tab on the online summary pages for acoustic noise.

3 Progress of Work

3.1 Weeks 1-2

I learned how to generate the current format of summary pages from both the 40m lab computers and the LIGO clusters. I gained a knowledge of the command line tools for summary page generation and use of configuration files. I also learned how to write my own configuration files and added a tab to the main Caltech 40m summary pages to display a suspension coil voltage monitor. Additionally, I learned how to create tabs based on external html pages, a tool which is used later for creating a screen capture tab for the MEDM status screens. Various amounts of data were tested and pages were created from both Caltech 40m and Livingston site data. Additionally, HTML5, XML, and JavaScript were all learned

at a basic level, which enabled me to continue forward in developing an external webpage for the MEDM tab. Figure 3 shows an example plot from the new voltage monitor tab that has been incorporated into the main summary pages.

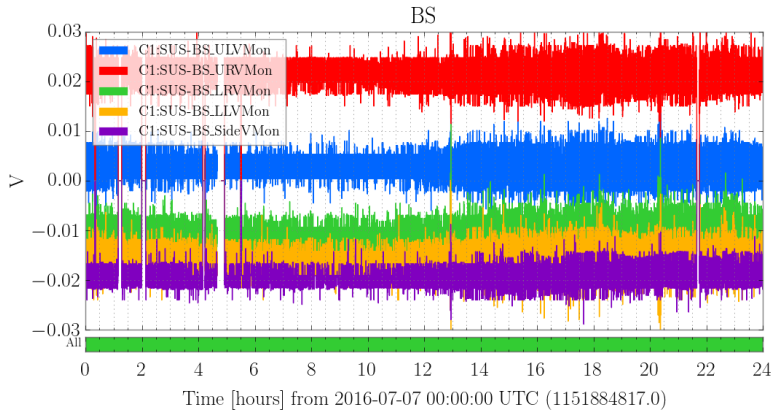

Figure 6: Beam splitter (BS) suspension coil voltage monitor from July 7, 2016 page [12].

3.2 Weeks 3-5

During these three weeks, I implemented an MEDM screen tab onto the online summary pages. This tab displays some the screens that researchers at the 40m find most useful and updates every 10 minutes with a cronjob. A screenshot of this new tab is given below.

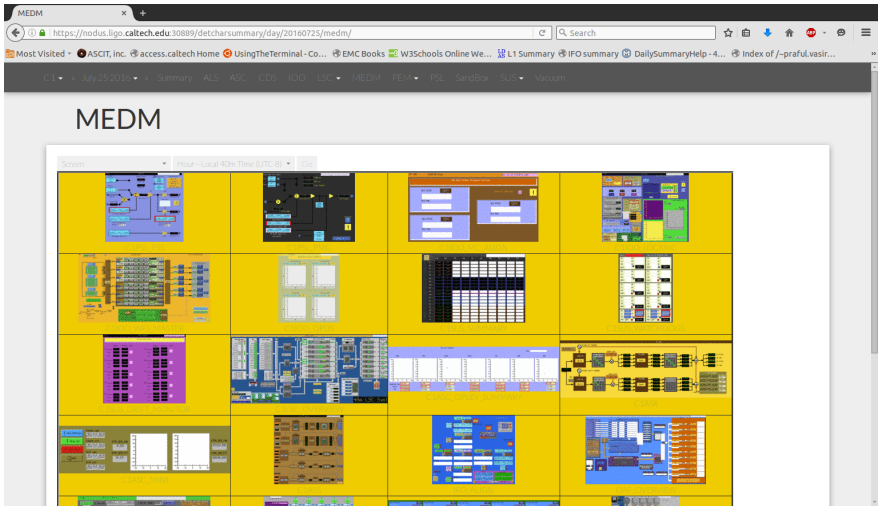

Figure 7: New MEDM tab on online summary pages. The page displays important screens and includes an archive lookup system to search for a particular screen on a given day.

The main difficulties in implementing this MEDM screen tab were setting up the cronjob, which schedules when to run the scripts to capture the MEDM screens, and configuring the virtual display of the screens. These issues were solved through ensuring that terminal environment variables were set up correctly and explicitly specifying the locations of windows in the virtual display so that the screen capture scripts could find the desired MEDM screens.

3.3 Weeks 6-10

3.3.1 Initial Problems and New Circuit

Next, I began to work on designing a system to cancel acoustic noise from the interferometer readout. After initially setting up the original microphone amplifier circuit shown in Section 2.3.3, I noticed some clipping issues in the signal through the amplifier. Though the circuit was fed in a sinusoid from a function generator, the output would be a truncated and amplified sinusoid. I attempted to fix this issue by adding a negative input voltage to pin 4 on the opamp. This new addition fixed the clipping issue and produced amplified sinusoids after again being given input from a function generator. However, when the microphone was attached to this new circuit, I ran into more problems such as incorrect voltage readouts along resistors and the output not actually being amplified. I decided to try implementing a different, simpler amplifier circuit to see if my problems could be fixed. The new circuit that I have implemented is shown below. This circuit satisfies the design requirements of the previous circuit from which I could not obtain an accurate transfer function. These requirements include a high-pass filter at 7 Hz and a low-pass filter with a cutoff frequency of 23 kHz. The rolloff, or the steepness of the decline of the gain at frequencies outside of the passband, can be adjusted as well.

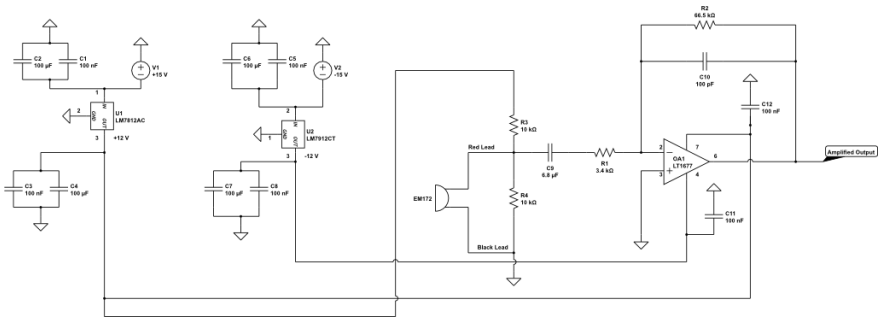

Figure 8: New amplifier circuit to be implemented. This circuit includes negative input to pin 4 and includes bypass capacitors from the voltage supplies and power regulators.

Using this circuit, I was able to successfully amplify microphone input, such as sinusoid tones from audio generators. This circuit can be easily changed to include different cutoff frequencies and increase or decrease the gain by changing the values of the resistors and capacitors. I also verified that the passband of the amplifier circuit works as expected by measuring the transfer function. I have set a high-pass filter at 7 Hz and a low-pass filter at 23 kHz.

3.3.2 Results of New Circuit

The transfer function of this new, simpler circuit, is given below.

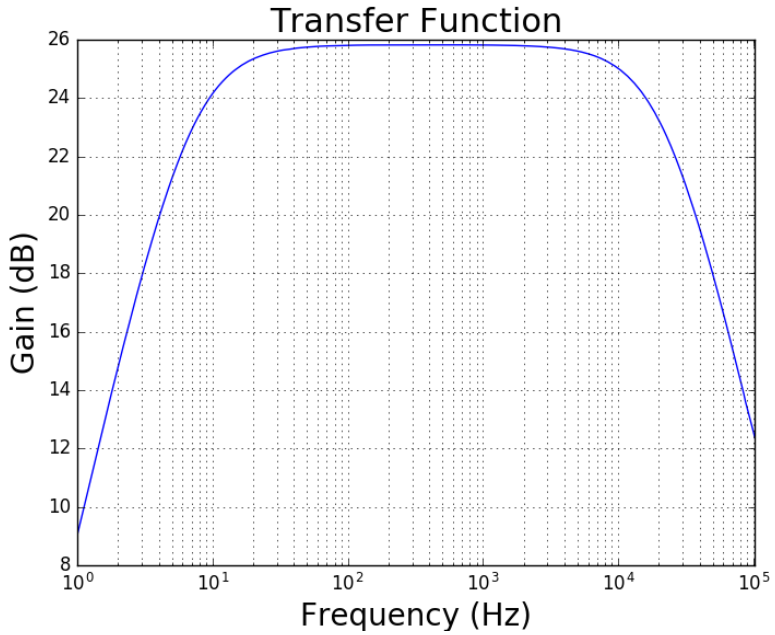

Figure 9: Transfer function of new inverting amplifier circuit. The passband worked as expected with a decrease in gain at frequencies smaller than 7 Hz and larger than 23 kHz.

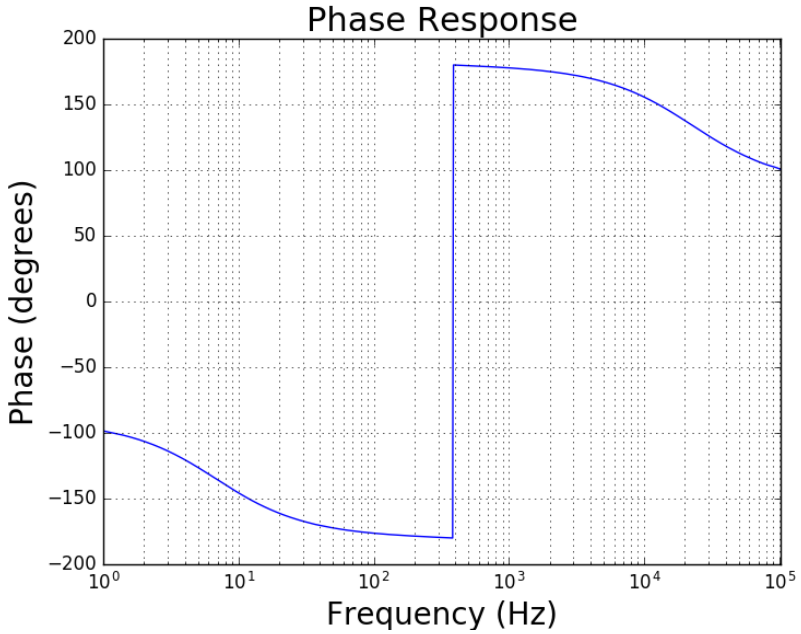

Figure 10: Phase response of new inverting amplifier circuit.

3.3.3 Isolating the Acoustic Signal

In order to perform more accurate noise cancellation, the readout from the microphone must be separated into the true acoustic signal, which will be used in noise cancellation, and electronic and mechanical noise, or self noise, resulting from the microphone itself. The preliminary attempt at accomplishing this involved setting up the amplifier-microphone

system in a box filled with foam. The goal of this setup was to block the lab acoustic signal from the microphone and thus study the baseline noise generated by the microphones' electronic and mechanical properties. The spectra inside and outside this setup are given below.

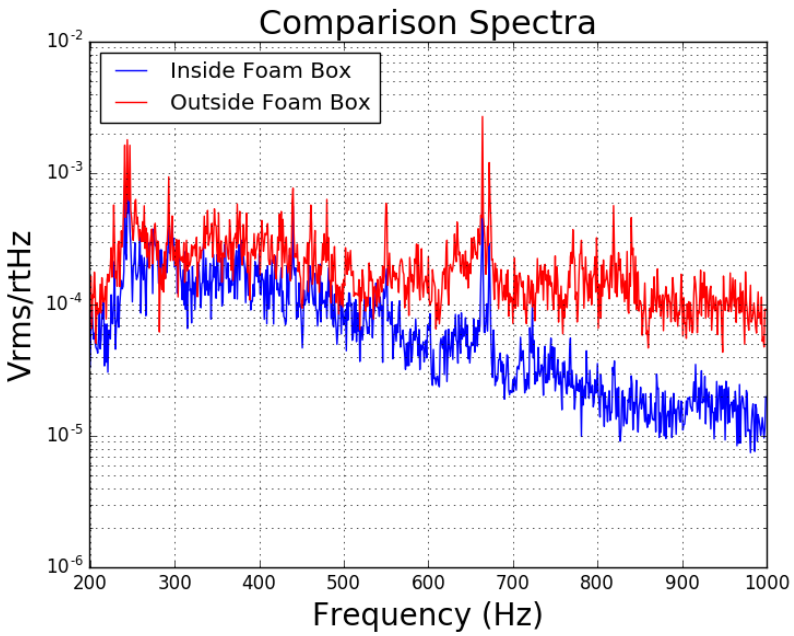

Figure 11: Spectrum of EM172 microphone inside and outside foam box. The two major frequency peaks are at about 250 Hz and 650 Hz.

However, as can be seen in the comparison spectra in Figure 11, the foam box did not greatly shield the microphone. Therefore, a new method was needed in order to isolate the microphone's self noise.

The basic idea behind the new method used to isolate the microphone self noise is as follows: if multiple microphones are placed close enough together such that they receive nearly the exact same true acoustic signal, this signal will be shared in the readout of all microphones with the only variation between them being the self noise of each individual microphone. As all of the microphones are designed by the same manufacturer, it is expected that the amplitude of the self noise in each microphone will be nearly the same. However, the self noise will vary in phase among the microphones because this noise is caused by random electronic and mechanical sources. This method, a frequency-dependent measurement of the multi-coherence between the microphones, requires at least two sensors, a target and witness(es) and accounts for the correlation between the target and each witness as well as between witnesses. Coherence in this context refers to the fraction of the signal power that is self noise or true acoustic signal in the frequency domain. This method measures the coherence of the self noise in different frequency bins. The results of this method are given below.

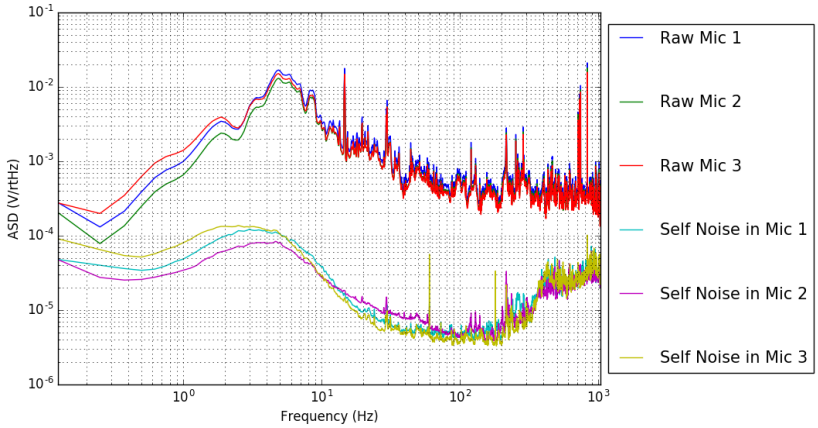

Figure 12: Amplitude spectral density of readout of three microphones placed very closed together and self noise of each microphone.

As expected from microphones of the same manufacturer, the amplitude of the self noise is similar among all three microphones. This separation of self noise from readout is achived by studying the incoherent phase relationship between the self noises of the microphones. This separation of self noise from true acoustic signal will be used in order to ensure more accurate acoustic noise cancellation.

3.3.4 Prototype Box and PEM-Acoustic Tab on Summary Pages

Next, I created a prototype box with my circuit inside to be suspended in the PSL table to ensure that everything is working as expected. Some pictures of this prototype are given below.

Figure 13: Outside view of the prototype box. The circuit is connected to a BNC connector for data readout and a three pronged power supply.

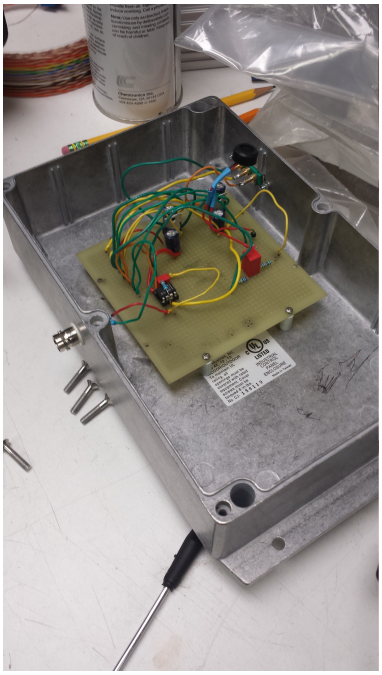

Figure 14: Inside view of prototype box.

This box was then suspended inside the PSL table and connected to a data channel. This data channel was then put on the summary pages in a new tab.

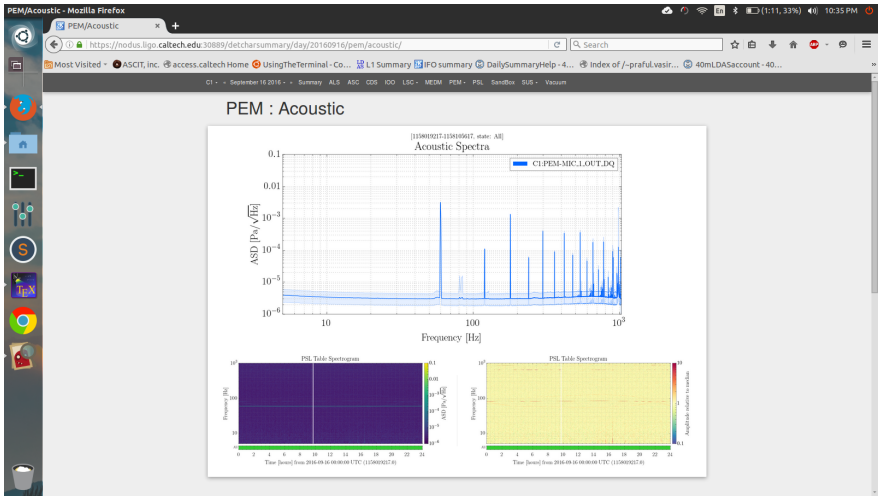

Figure 14: New PEM-Acoustic tab on summary pages. A spectrum is given at the top from the channel along with a spectrogram and whitened spectrogram.

In the future, the plan is that the top plot will display multiple spectra from microphones set up at different locations along the interferometer. Additionally, each row after the top spectra will be a spectrogram and whitened spectrogram from each individual microphone. The box is currently unpowered so all data so far is just electronics noise. Thus, the data shown on the current tab is just the result of mains hum from alternating current.

4 Conclusions and Future Work

Overall, this summer I succeeded in adding an MEDM tab to the online summary pages, creating a new circuit which fulfills the design requirements, and making a prototype box. Some future work that I will work on in the Fall involves sending the circuit design to a manufacturer for fabrication, making a large number of amplifier-microphone system boxes, and suspending them around the interferometer. In order to fully optimize the locations of the microphones, machine learning could be used in order to most effectively study the coupling of acoustic noise to the differential arm length channel readout. This sort of machine learning program would be useful not only in this acoustic noise project but also for any sensor array at the interferometer.

5 Acknowledgements

I sincerely thank my mentors, Maximiliano Isi, Gautam Venugopalan, and Rana Adhikari, as well as everyone who helped me at the 40m over the summer, including Eric Quintero, Steve Vass, Koji Arai, Lydia Nevin, Aakash Patil, and Varun Kelkar. I also want to thank Yoichi Aso for his help in getting the MEDM scripts working properly.

6 References

[1] Abbott, B.P. et al (2016). Observation of Gravitational Waves from a Binary Black Hole Merger. Physical Review Letters, 116 (061102).

[2] Abbott, B.P. et al (2016). Characterization of transient noise in Advanced LIGO relevant to gravitational wave signal GW150914.

[3] Christensen, Nelson (2010). LIGO S6 detector characterization studies. Classical and Quantum Gravity, 27 (194010).

[4] Working with gravitational wave data. https://gwpy.github.io/docs/stable/index.html

[5] Adhikari, Rana (2004). Sensitivity and Noise Analysis of 4 km Laser Interferometric Gravitational Wave Antennae. Massachusetts Institute of Technology.

[6] What is an interferometer? https://www.ligo.caltech.edu/page/what-is-interferometer

[7] Abbott, B.P. et al (2009). LIGO; the Laser Interferometer Gravitational-Wave Observatory. Reports on Progress in Physics, 72(7).

[8] `gwsumm`. https://github.com/gwpy/gwsumm

[9] L1 Hierarchical Veto. https://ldas-jobs.ligo-la.caltech.edu/~duncan.macleod/hveto/day/20151225/

[10] SVG. https://developer.mozilla.org/en-US/docs/Web/SVG

[11] PEM: Seismic. https://nodus.ligo.caltech.edu:30889/detcharsummary/day/20160707/pem/seismic/

[12] Suspension coil voltage monitor (VMon). https://nodus.ligo.caltech.edu:30889/detcharsummary/day/20160707/sus/vmon/

[13] L1 Hierarchical Veto, December 25th, 2015. https://ldas-jobs.ligo-la.caltech.edu/~duncan.macleod/hveto/day/20151225/plots/L1-HVETO_SIG_DROP_ROUND_1-1135036817-86400.svg

[14] A whistle-stop tour of the INI format. https://ldas-jobs.ligo.caltech.edu/~duncan.macleod/gwsumm/latest/configuration/format.html